

Han, D., Patrikakis, V., and Barakos, G. N. (2016) Helicopter flight performance improvement by dynamic blade twist. *Aerospace Science and Technology*, 58, pp. 445-452. (doi:[10.1016/j.ast.2016.09.013](https://doi.org/10.1016/j.ast.2016.09.013))

This is the author's final accepted version.

There may be differences between this version and the published version. You are advised to consult the publisher's version if you wish to cite from it.

<http://eprints.gla.ac.uk/128135/>

Deposited on: 13 September 2016

# Helicopter Flight Performance Improvement by **Dynamic** Blade Twist

**Dong Han**

National Key Laboratory of Science and Technology on Rotorcraft Aeromechanics, College of Aerospace Engineering,  
Nanjing University of Aeronautics and Astronautics, Nanjing 210016, Jiangsu, China

**Vasileios Pastrikakis and George N. Barakos**

School of Engineering, University of Glasgow, G12 8QQ, Scotland, U.K.

**Dynamic** blade twist is investigated as a method for reducing rotor power and improving helicopter performance. An analytical model able to predict helicopter rotor power is first presented, and the flight data of the UH-60A helicopter and the Helicopter Multi-Block Method (HMB2) are used for validation. The predictions of the rotor power are in good agreement with the flight test data and HMB2, which verifies the application of the present method in analyzing helicopter performance. In hover and low speed forward flight, the power reduction by the prescribed **dynamic** blade twist is substantially small. In high speed forward flight, the effect of **dynamic** blade twist becomes more pronounced. It is found that lower harmonic blade twist can achieve larger power savings than higher harmonic twist. The zero harmonic twist dominates the power reductions. The helicopter take-off weight was found to have a strong influence on the power reductions achieved by the prescribed **dynamic** blade twist.

Keywords: helicopter; flight performance; **dynamic** blade twist; periodic harmonic twist

## 1. Introduction

Negative blade twist can improve helicopter rotor efficiency in hover and forward flight [1, 2]. It has been widely applied in rotor blade design to achieve better helicopter rotor performance [3-5] by optimizing the distribution of blade lift and reducing the rotor power. This effect is achieved by increasing the loading inboards along the blade. Blade twist can also delay blade stall at high forward speeds and mitigate compressibility effects at high tip speeds [1], since blade twist unloads the tips by reducing the tip angle of attack. Usually, passive pre-twist is used along the blade span, which cannot actively change around the azimuth. To accommodate the asymmetric aerodynamic environment of the blade at the retreating and advancing sides in forward flight, a change of the spanwise and azimuthal twist distributions is needed.

Currently, actively changing blade twist has not been applied in helicopter rotor design. This is partly due to difficulties with the required mechanism for the twist change and the manufacturing of this new breed of rotor blades. In recent years, piezoelectric materials have been used to actuate the blade twist [6, 7], like active fiber composites (AFC) [8-10] and macro fiber composites (MFC) [11-13]. Smart materials and structures have demonstrated their potential in actuating blade twist and controlling rotor vibration loads, as well as, improving helicopter rotor performance. Yeo [14] investigated different active controls for rotor performance improvement. The 1/rev (per revolution) active blade twist had a small influence on the rotor performance, and the 2/rev harmonic control was found to improve the rotor lift-to-drag ratio. The benefit studies of an active twist rotor conducted by Zhang et al. [15] using a weak fluid-structure coupling method resulted in power reduction of about 14%. This value was probably overestimated, however, the numerical results showed clearly the performance improvement achieved by the active twist control. Body Jr. utilized a loosely coupled CFD/CSD (computational fluid dynamics/ computational structural dynamics) method to analyze the aerodynamic and acoustic performance of an active twist rotor [16]. The 3/rev input reduced both mid-frequency noise and 4/rev hub vibrations with a penalty in the rotor lift-to-drag ratio. Kang et al. investigated different rotor morphing technologies for helicopter performance improvement [17]. The quasi-steady blade twist gave a 2% savings in the total

rotor power in cruise. Jain et al. investigated three rotor morphing concepts for performance improvement [18], namely trailing-edge deflection, leading-edge deflection and active twist. The predictions by the CFD and CSD coupling for the UH-60A rotor showed that the active twist reduced the power in high speed flight (C8534) by 3.3% but no reduction was found for the high thrust flight (C9017). The examinations of on-blade active controls conducted by Jain et al. illustrated that the 2/rev input with the optimal amplitude of 4 degree of active twist could reduce the rotor power by 3.3% in high speed forward flight [19]. The previous analyses concentrate on rotor performance improvements by changing the blade static twist (pre-twist) without any dynamic twist or the dynamic twist based on prescribed static twist.

A blade twist can contain static, active and elastic components. One, two, or all three components may affect rotor performance. How to find the major factors dominating the performance improvement is a very challenging and worthy research area. Essentially, any a blade twist, which is a sum of the static, active and elastic twists, can be expressed as a sum of the components from 0/rev to  $+\infty$ /rev. If we can determine which harmonic twist dominates the performance improvement, active blade twist can be designed for optimized performance.

In this work, the blade twist is prescribed in the spanwise direction and around the azimuth, and investigated to determine which harmonic component (0/rev, 1/rev, ...,  $n$ /rev, ...) dominates the improvement in rotor performance. A helicopter rotor power prediction model is used, which includes a rigid blade model (suppress the effect of elastic twist), aerofoil table look-up method, the Pitt-Peters inflow model [20], a rigid fuselage model and a propulsive trim method [21]. The flight data of the UH-60A helicopter [22] is utilized to validate the model. The Helicopter Multi-Block Method (HMB2) [23, 24, 25] CFD method is also utilized to verify the analytical method. HMB2 has been validated for a range of rotorcraft applications and has demonstrated good accuracy and efficiency for very demanding flows. Examples of work with HMB2 can be found in references [23, 24, 25]. The zero harmonic twist combined with a periodic harmonic twist is analyzed to explore the potential of spanwise and azimuthal distribution of blade twist in saving rotor power and improving helicopter performance.

## 2. Modeling and Validation

To determine the dominant harmonic components of blade twist for minimum rotor power, a parameter sweep for each flight state, at a prescribed forward flight speed is conducted. This process has to be repeated for several rotor power settings. If one computation requires a CPU of one minute, the sweep of the parameters can span dozens of days. Since the objective of this work is to explore the potential of the harmonic component of **dynamic** blade twist in reducing rotor power, an analytical model to predict the helicopter rotor power is utilized. This model can estimate the rotor power within less than a second using a standard personal computer.

The blade model is based on a rigid beam with a hinge offset and a hinge spring, which is used to match the fundamental flapwise blade frequency. Look-up table aerofoil aerodynamics is used to calculate the lift and drag coefficients of blade elements according to the local resultant air flow and angle of attack. The induced velocity over the rotor disk is predicted by the Pitt-Peters inflow model [20], which captures the first harmonic variation of induced velocity in azimuth. The hub forces and moments of the main rotor are derived from the resultant root forces and moments of the blades. The fuselage is treated as a rigid body with specified aerodynamic forces and moments. For simplicity, the thrust of the tail rotor is determined by the main rotor torque divided by the distance from the hub center of the tail rotor to the main rotor shaft. The power and collective pitch of the tail rotor are determined by the thrust according to momentum theory.

Given three pitch controls (collective and two cyclics) and two rotor shaft attitude angles (longitudinal and lateral tilts), the periodic response of the rotor in steady forward flight can be obtained for a prescribed forward speed. The hub forces and moments of the main rotor are balanced by the forces and moments acting on the fuselage and tail rotor. The forces and moments on the fuselage are determined by the flight state and attitude angles. The thrust and power of the tail

rotor are derived from the rotor torque and flight state. These component forces and moments constitute the equilibrium equations of the helicopter [21], which are solved to update the pitch controls and rotor attitude angles for the next iteration. After several iterations of the periodic rotor responses and solutions of the equilibrium equations, the converged or trimmed pitch controls and rotor attitude angles can be obtained. Then the main rotor power and related information of the helicopter can be derived.

The flight data of the UH-60A helicopter [22] is utilized to validate the methodology used in this work. The parameters of the main rotor and tail rotor are listed in Table 1 and Table 2 [26]. The distributions of the airfoil and blade pre-twist of the main rotor are given in [27]. For the performance analysis, only the aerodynamic drag force is considered in the fuselage model. The fuselage drag equation utilized in the present analysis is [22]

$$\frac{D}{q} \text{ (ft}^2\text{)} = 35.83 + 0.016 \times (1.66\alpha_s^2) \quad (1)$$

where,  $D$  is the fuselage drag,  $q$  is the dynamic pressure, and  $\alpha_s$  is the aircraft pitch angle. The distance from the hub center of tail rotor to the rotor shaft is 9.9263 m. The vertical distance from the mass center of the helicopter to the rotor hub is 1.77546 m. The comparisons of the prediction of the rotor power with the flight test data for the takeoff weight coefficients 0.0065 and 0.0074 are shown in Figure 1. It is obvious that the predictions by the present method are generally in good agreements with the flight test data for these takeoff weights, which verifies the application of present method for the analysis of helicopter performance.

Table 1: Main rotor parameters

Main Rotor Radius	8.1778 m
Main Rotor Speed	27.0 rad/s
Blade Chord Length	0.5273 m
Blade Twist	Nonlinear
Blade Airfoil	SC1095/SC1094R8
Number of Blades	4
Flap Hinge Offset	0.381 m
Blade Mass per Unit Length	13.92 kg/m
Longitudinal Shaft Tilt	3°

Table 2: Tail rotor parameters

Tail Rotor Radius	1.6764 m
Tail Rotor Blade Chord	0.2469 m
Tail Rotor Speed	124.62 rad/s
Tail Rotor Blade Twist	-18°
Blade Airfoil	NACA0012
Number of Blades	4

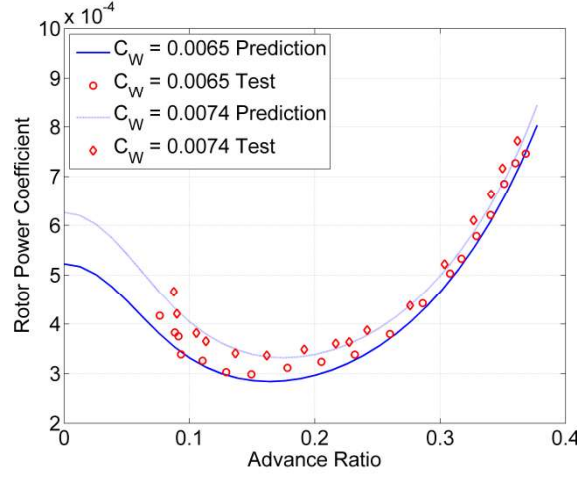


Figure 1 Comparison of predictions with flight test data.

### 3. Performance Analysis

The zero and a periodic harmonic twists are prescribed for rotor blades to improve helicopter rotor performance. The UH-60A rotor in the previous section is used as the baseline rotor with the modification of blade twist. Different harmonic components are analyzed to investigate the harmonic parameters of blade twist for rotor power savings.

#### 3.1 Strategy of Dynamic Blade Twist

The **dynamic** blade twist is prescribed to be linearly distributed along the spanwise (by  $r/R$ ) and azimuthal (by  $\psi$ ) directions as

$$\theta = \theta_0 + \theta_{1c} \cos \psi + \theta_{1s} \sin \psi + \theta_{tw} \frac{r}{R} \quad (2)$$

with the following blade twist law

$$\theta_{tw} = A_0 + A_n \cos(n\Omega t + \phi) \quad (3)$$

where,  $\theta_0$  is the collective pitch angle,  $\theta_{1c}$  is the lateral cyclic pitch angle,  $\theta_{1s}$  is the longitudinal cyclic pitch angle,  $r$  is the radial location,  $R$  is the rotor radius,  $A_0$  denotes the amplitude of 0/rev twist,  $A_n$  denotes the amplitude of the  $n$ /rev harmonic component,  $n$  is the harmonic number, and  $\phi$  is the corresponding phase angle. The complete **dynamic** blade twist equation is

$$\theta = \theta_0 + \theta_{1c} \cos \psi + \theta_{1s} \sin \psi + \frac{r}{R} [A_0 + A_n \cos(n\Omega t + \phi)] \quad (4)$$

The amplitudes of 0/rev and  $n$ /rev twists are prescribed in integer values only. The harmonic inputs  $n$  are also integer values.  $A_0$  varies between  $-25^\circ$  and  $0^\circ$ , and  $A_n$  between  $0^\circ$  and  $20^\circ$ . The phase angle  $\phi$  can vary from  $0^\circ$  to  $360^\circ$  with  $5^\circ$  increment. With the limits of these parameters, the rotor responses are calculated over all the cases to determine the minimum rotor power for different harmonic components. If the periodic responses cannot achieve convergent solutions, or the parameters of blade twist corresponding to the minimum value fall out of the boundaries, the prescribed limits of the parameters are changed for the search of the minimum rotor power.

The power reduction ratio is defined to determine the benefit in rotor power savings as

$$\eta = (1 - P/P_b) \times 100\% \quad (5)$$

where,  $P$  is the rotor power with the prescribed **dynamic** blade twist and  $P_b$  is the baseline rotor power.

### 3.2 First Harmonic Twist

To assess the effect of blade twist in reducing rotor power, some baseline rotor powers are needed as reference. Since linear variation of blade twist is used in this work, some passive prescribed blade twists ( $-20^\circ$ ,  $-16^\circ$ ,  $-12^\circ$  and  $-8^\circ$ ) without periodic harmonic component are utilized as the baseline cases. A helicopter weight coefficient 0.0065 is used in the discussion of the different harmonic components.

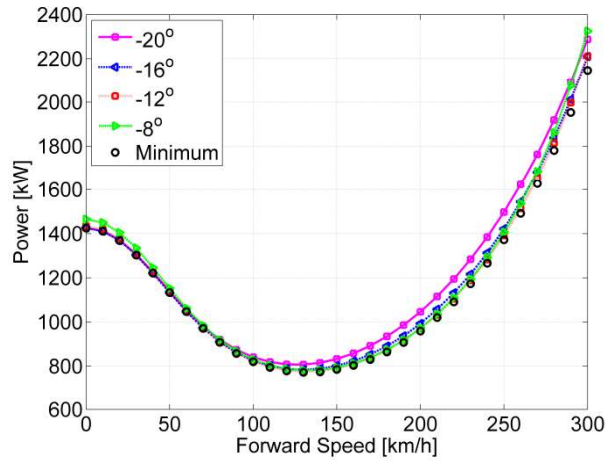


Figure 2 Power comparisons for 1/rev blade twist.

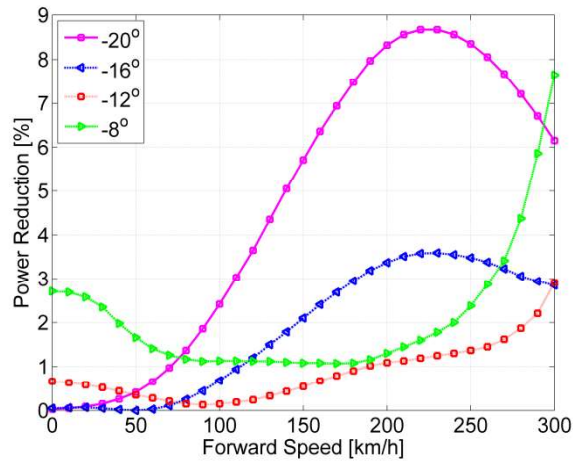


Figure 3 Power reductions by 1/rev blade twist.

Figure 2 shows the comparisons of the minimum rotor power with the baseline powers for different forward speeds. These minimum powers are determined by the simultaneous parameter sweep of the 0/rev and 1/rev twists. Figure 3 shows the corresponding power reduction ratios. Compared with the prescribed  $-12^\circ$  twist, the maximum power reduction is 2.91% at a speed of 300 km/h. The effect on the power savings is substantially small, especially considering the power consumption required for the twist actuation. The maximum power reduction is 8.67% at a speed of 230 km/h if

compared with the power of the prescribed  $-20^\circ$  twist. It is obvious that the design of the passive spanwise pre-twist has distinct influence on the power savings. At low speed forward flight, the reductions are, overall, substantially small. With increasing forward speed, the effect becomes more pronounced. The maximum power reductions emerge at medium to high speeds. This means that, varying blade twist is suitable for medium to high speed forward flight, and it is not very effective in hover and low speed flight.

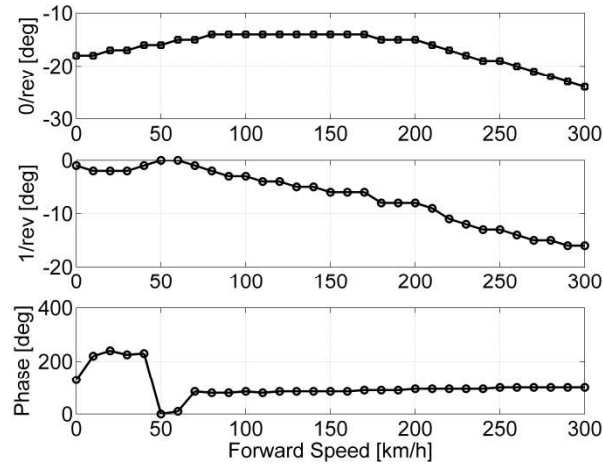


Figure 4 0/rev and 1/rev twists.

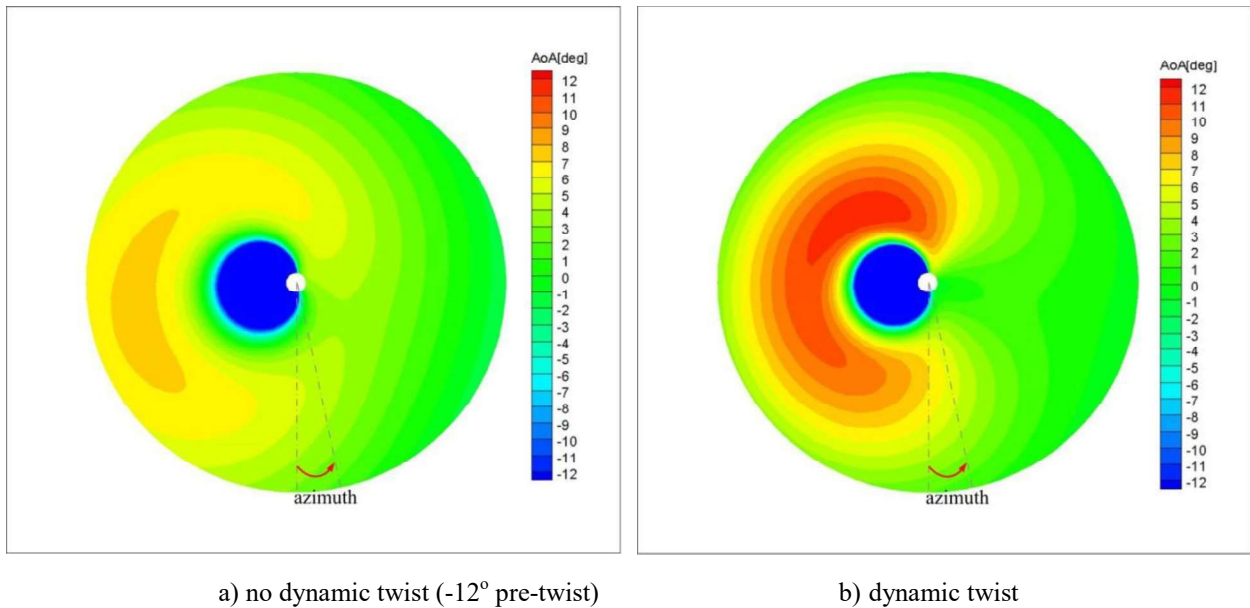


Figure 5 Distribution of angle of attack (230 km/h).

The 0/rev twist, 1/rev twist and phase angle of the 1/rev twist corresponding to the minimum rotor powers for different forward speeds are shown in Figure 4. Large 0/rev blade twist and small 1/rev twist are preferred in hover and low forward speed. With increasing forward speed, the 0/rev twist decreases and the 1/rev twist increases. Then, at even higher speeds, the 0/rev twist increases and the 1/rev twist still increases, which is used to alleviate the asymmetric aerodynamic environment. It is to be noted that large 0/rev and 1/rev twists are needed for high speed forward flight, and this may cause problems with the twist actuation. In hover, and low speed forward flight, the phase angle changes abruptly. In these cases, the amplitudes of the corresponding 1/rev twist are very small. If the speed is larger than 70

km/h, the phase angle varies between  $85^\circ$  and  $100^\circ$ . The variation is substantially small. Figure 5 shows a comparison of the distribution of the angle of attack over the rotor disk at a speed of 230 km/h. It is obvious, that the retreating side has been significantly **optimized**. With the **dynamic** blade twist, the angle of attack of the retreating side shifts inboards and increases. Since the airfoil SC1095 near the blade tip is not of a high-lift type, the shift of the lift to the inner airfoil SC1094R8 can increase the rotor lift-to-drag ratio and decreases the rotor power.

The parameter sweep of the prescribed blade twist includes two components: 0/rev and 1/rev twists. The cases corresponding to the maximum and minimum power reductions are those with the pre-twist  $-20^\circ$  and  $-12^\circ$ , which are utilized to analyze the contributions to the power reductions from the two twists. Figure 6 shows the maximum power reductions compared with the  $-20^\circ$  and  $-12^\circ$  linear pre-twist. The ‘0/rev + 1/rev’ in the figure denotes the power reductions are obtained by the parameter sweep of  $A_0$  and  $A_1$ , and the ‘0/rev’ denotes the reductions by the parameter sweep of  $A_0$  only. It is obvious that the combined 0/rev and 1/rev twists can achieve larger rotor power reductions than the 0/rev twist. The difference increases with the forward speed, generally. The reductions between the combined and individual twists at the forward speed 300 km/h are 2.21% and 2.28% for the  $-20^\circ$  and  $-12^\circ$  pre-twist, respectively. From the case with the  $-20^\circ$  pre-twist, it is obvious that the 0/rev twist contributes most part of the power savings. The combined 0/rev and 1/rev twists can obtain substantially small increase of power reductions. In hover and low speed forward flight, the values of power reductions by the two schemes of blade twist are almost the same, which means that the 1/rev twist is not necessary to be utilized in these flight states. The 1/rev twist appears to be more suitable for medium to high forward speeds.

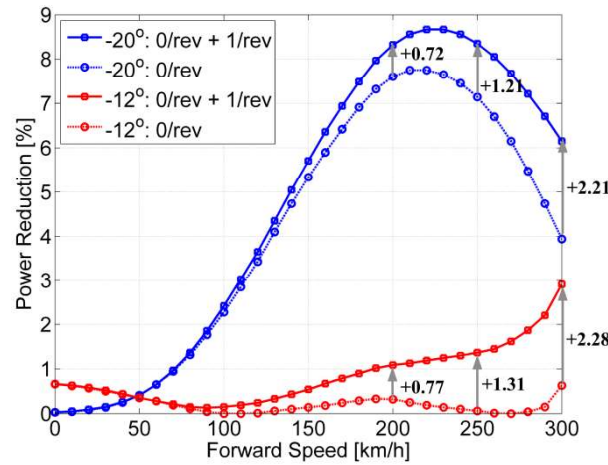


Figure 6 Power reductions by 1/rev active twist and static twist.

### 3.3 Second Harmonic Twist

Figure 7 shows the comparisons of rotor powers, and the minimum power. The figure is obtained by a parameter sweep of the 0/rev and 2/rev twists. Figure 8 shows the corresponding power reductions. In hover and low forward flight, the power reductions are substantially small, but, in medium to high speed flight, the effect becomes pronounced. It is obvious that the overall power reductions are substantially small (not larger than 3.21%) with the baseline pre-twists  $-12^\circ$  and  $-16^\circ$ . For the pre-twists of  $-8^\circ$  and  $-20^\circ$ , the power reductions are 7.0% and 5.49% at a speed of 300 km/h. The combined 0/rev and 2/rev twists can achieve better rotor power savings and rotor performance improvement in high speed flight, which is due to the change of the baseline pre-twist.

The 0/rev twist, 2/rev twist and phase angle of the 2/rev twist corresponding to the maximum power reductions for different forward speeds are shown in Figure 9. In hover, and low speed forward flight, the 2/rev twist is zero. The power



reductions are therefore originating from the change of the 0/rev twist. At speeds from 130 km/h to 300 km/h, the amplitude of the 2/rev twist is  $1^\circ$ . This small 2/rev amplitude may achieve a limited rotor power reduction. The phase angles corresponding to these speeds are near  $0^\circ$ .

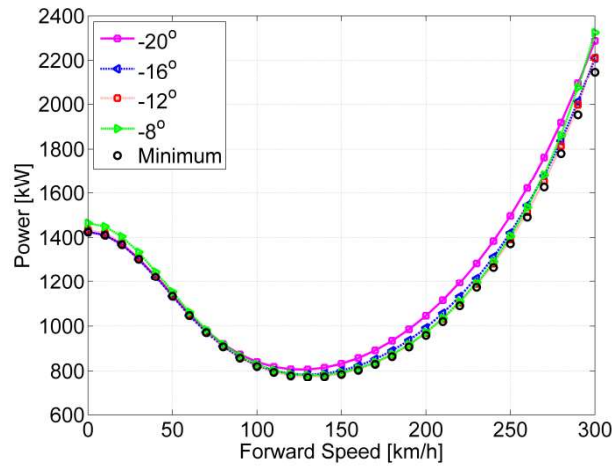


Figure 7 Power comparisons for 2/rev blade twist.

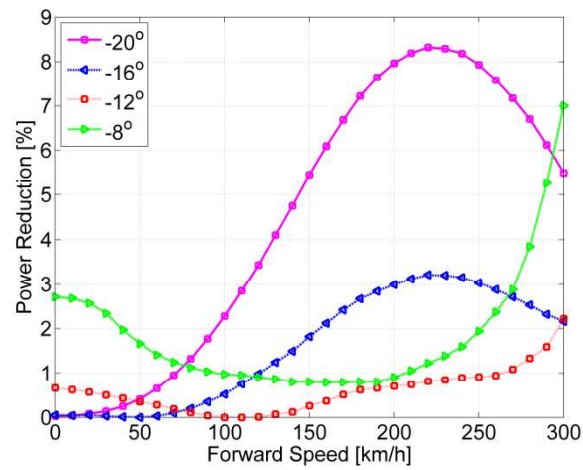


Figure 8 Power reductions by 2/rev blade twist.

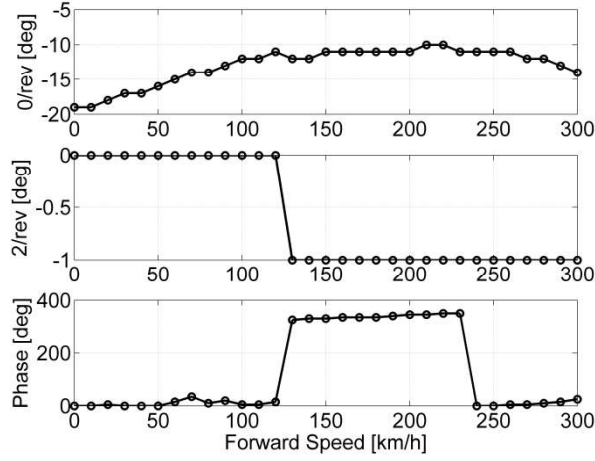


Figure 9 0/rev and 2/rev twists.

Figure 10 shows the maximum power reductions by the 0/rev twist with and without the 2/rev twist for the cases compared with the  $-12^\circ$  and  $-20^\circ$  cases of linear pre-twist. At a speed of 200 km/h, the differences are 0.38% and 0.36%. The differences increase to 1.59% and 1.55% at a speed of 300 km/h. These savings from the 0/rev twist to the combined 0/rev and 2/rev twists are rather small. It is not necessary to utilize the 2/rev twist to obtain power savings. Compared with Figure 6, the 1/rev twist can achieve larger power reductions than the 2/rev twist, which means the 1/rev blade twist is more effective.

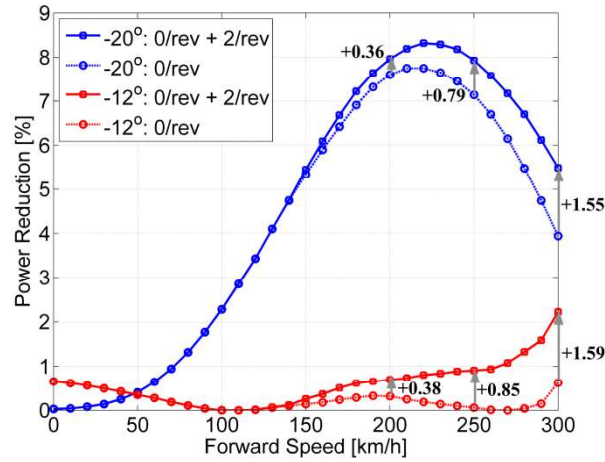


Figure 10 Power reductions by 2/rev twist and/or 0/rev twist.

### 3.4 Higher Harmonic Twist

Figure 11 shows the power reduction for the 3/rev blade twist, for different baseline pre-twists. The trends are similar as the 1/rev and 2/rev twists. However, the amplitudes of the power reductions are smaller. Figure 12 shows the corresponding 0/rev twist, 3/rev twist and phase angle of the 3/rev twist. It is obvious that the 3/rev twist doesn't work when the forward speed is less than 210 km/h. The amplitudes of 3/rev twist are  $1^\circ$  when the speed is larger than this speed. In high speed forward flight, the power reduction between the 0/rev twist with and without the 3/rev twist is less than 1.0% (compare with the 0/rev twist in Figure 6). This indicates that the 3/rev twist is not effective in reducing rotor power and improving helicopter rotor performance.

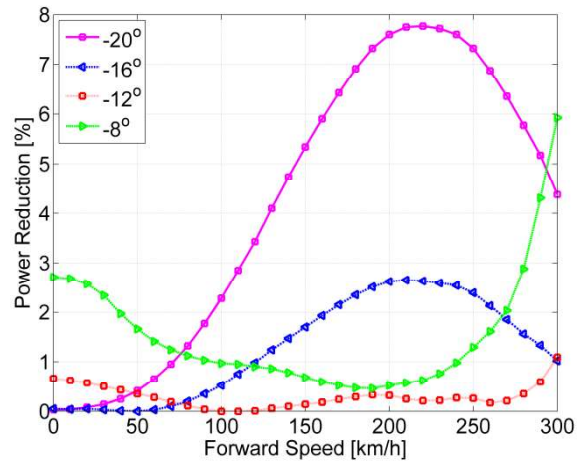


Figure 11 Power reductions by 3/rev blade twist.

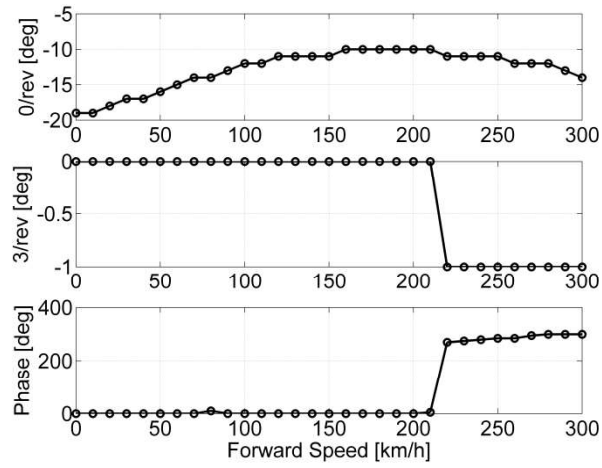


Figure 12 Static and 3/rev dynamic twist.

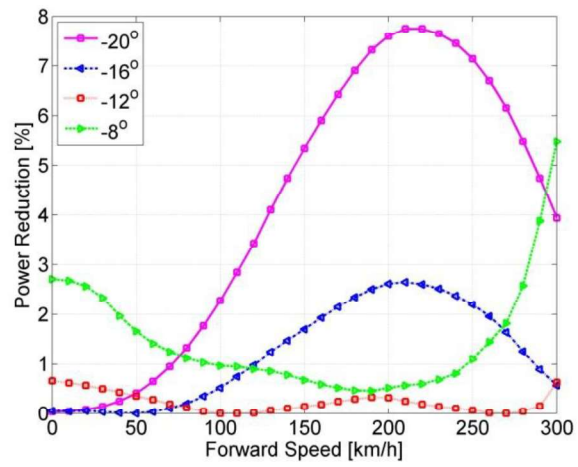


Figure 13 Power reductions by 4/rev input.

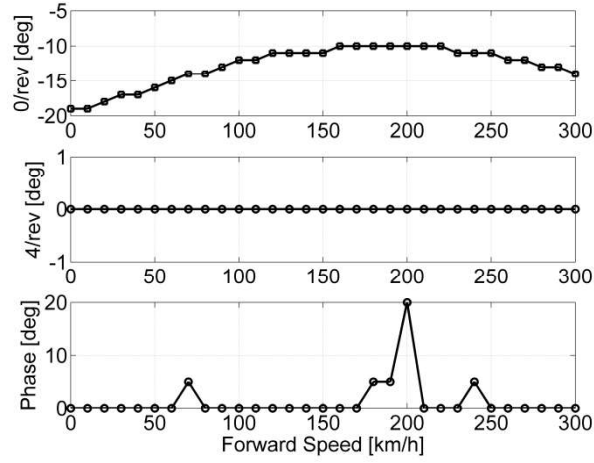


Figure 14 0/rev and 4/rev twists.

Figure 13 shows the power reduction by the 4/rev twist for different baseline pre-twists. The trends are similar as the previous harmonic twists. However, the amplitudes of the power reductions are smaller. Figure 14 shows the corresponding 0/rev twist, 4/rev twist and phase angle of the 4/rev twist. It is obvious that the 4/rev twist doesn't work over all speeds investigated. In hover, the required 0/rev twist is very large. With increasing forward speed, it decreases and then increases.

### 3.5 Comparisons with CFD method

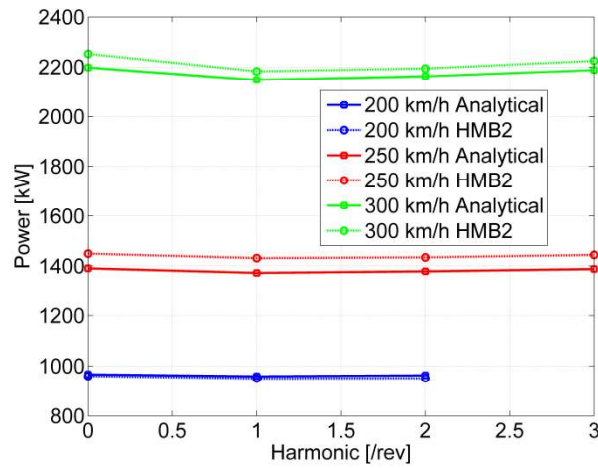


Figure 15 Comparison of rotor powers between empirical model and CFD model.

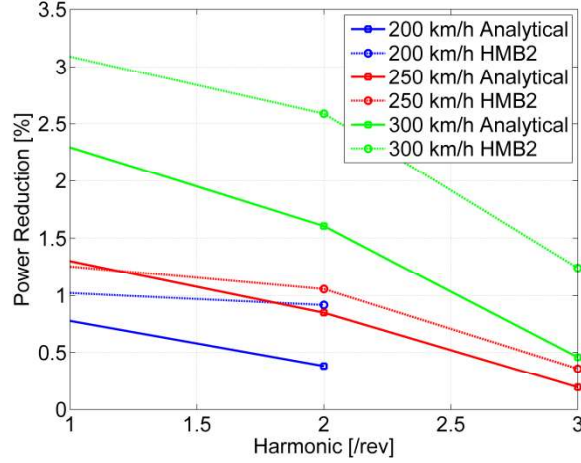


Figure 16 Comparison of power reductions between empirical model and CFD model.

To verify the analyses of blade twist, the CFD results generated by the Helicopter Multi-Block Method (HMB2) [23-25] are utilized for comparisons with the analytical method. The input of the twist to HMB2 is the same as the twists corresponding to the minimum power calculated by the analytical method. Figure 15 shows the comparison of rotor powers calculated by the analytical method and HMB2 for different harmonic twists at the speeds of 200, 250 and 300 km/h. The corresponding power reductions compared with the case at 0/rev twist as the baseline power are shown in Figure 16. It is clear that the results predicted by the two methods are in very good agreement. At a speed of 200 km/h, the absolute values of the rotor powers are almost the same. At a speed of 300 km/h, the differences are substantially small. In Figure 16, it is clear that the power reductions by the 1/rev twist compared with the 0/rev twist predicted by the two methods are 2.29% and 3.09% at a speed of 300 km/h. With decreasing forward speed, the reductions by the combined twists decrease. With increasing harmonic number, the power reductions decrease, which illustrates that higher harmonic components have a lesser effect on the rotor power savings. It also illustrates that periodic harmonic blade twist has small influence on the rotor power reduction, which is dominated by the 0/rev blade twist.

### 3.6 Larger Takeoff Weight

Figure 17 shows the power reductions by the 0/rev twist with a different periodic harmonic twist for a larger helicopter takeoff weight ( $C_w = 0.0074$ ). It is compared with the baseline pre-twist of  $-12^\circ$ . It is obvious that lower harmonic twist can obtain larger power savings than higher harmonic twist. In hover and lower forward flight, the different harmonic twists can achieve almost the same power reductions. With increasing forward speed, the power reduction first decreases and then increases, and in most forward speeds, the power reduction is less than 2.0%. The **dynamic** blade twist works better at high forward speed, and at a speed of 300 km/h, the power reductions by the 1/rev to 4/rev twists are 6.19%, 5.37%, 3.91% and 3.44%, respectively. These values are 2.91%, 2.22%, 1.09% and 0.63% for the weight coefficient of 0.0065. With increasing helicopter takeoff weight, the prescribed **dynamic** blade twist can achieve larger power reductions.

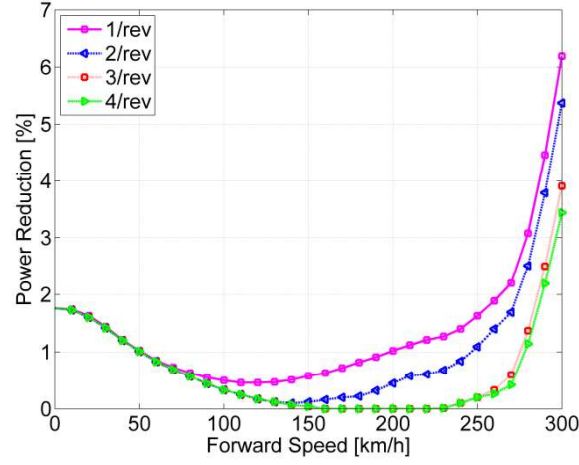


Figure 17 Power reductions with larger takeoff weight ( $C_w = 0.0074$ ).

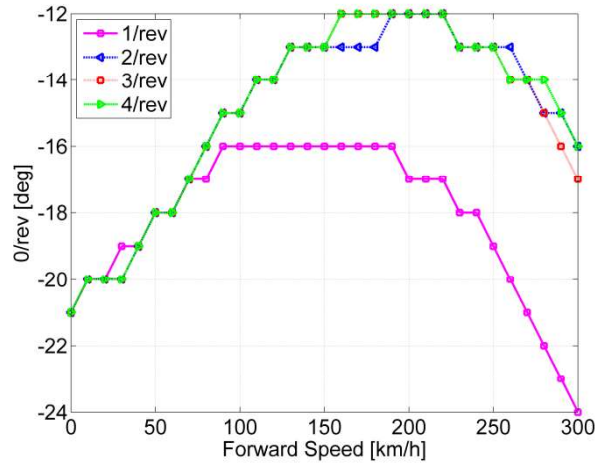


Figure 18 0/rev twists for different periodic harmonic twists ( $C_w = 0.0074$ ).

Figures 18 and 19 show the corresponding 0/rev and periodic harmonic twists. In hover, larger 0/rev twist is preferred, which is larger now than for the case with a smaller weight coefficient. With increasing speed, the twist decreases and then increases in high speed flight. For the 1/rev twist, a large 0/rev twist is needed in medium to high speed forward flight, which is obviously different from the other harmonic twist. This trend is the same for the periodic harmonic twist. For the 1/rev twist, the amplitude is small in hover, and low speed forward flight, but increases distinctly with forward speed. For the 2/rev and 3/rev twists, the periodic harmonic twist is small over the investigated speeds. For the 4/rev input, the periodic harmonic twist doesn't seem to work over the range of the investigated speeds. This shows to what was shown in Figure 14. From this figure, and Figure 17, the power reductions by the periodic harmonic twists are seen to be small.

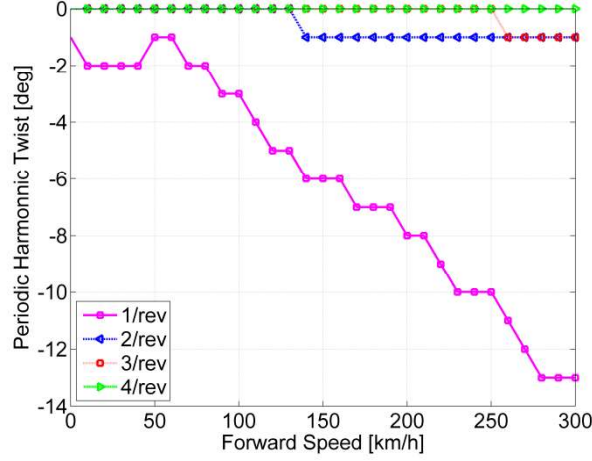


Figure 19 Periodic harmonic twists for different harmonic inputs ( $C_w = 0.0074$ ).

The previous analysis is based on the baseline pre-twist of  $-12^\circ$ . From Figures 18 and 19, this pre-twist is suitable for medium high forward flight. In high forward flight, larger pre-twist is preferred. If the baseline pre-twist is larger, for example  $-16^\circ$ , the power reductions for different harmonic twists at a speed of 300 km/h are 2.85%, 2.0%, 0.49% and 0.0%, respectively. With this pre-twist as the baseline, the active blade twist achieves smaller power reductions for the larger takeoff weight ( $C_w = 0.0074$ ), but larger reductions for the smaller takeoff weight ( $C_w = 0.0065$ ). It is obvious, that the initial design of the passive prescribed blade twist can accommodate some flight states, but not the overall flight envelope. Different flight states (speed, altitude, helicopter weight, maneuver, etc.), require different distributions of blade twist, which provides a wide space for the application of **dynamic** blade twist in improving helicopter performance.

#### 4. Conclusions

An analytical helicopter method was used to explore helicopter performance improvements by **dynamic** blade twist. The flight data of the UH-60A helicopter and the Helicopter Multi-Block Method (HMB2) were used to validate the method. The predictions of the rotor power by the analytical method are in good agreement with the flight test data and HMB2, which verifies the application of the present method in analyzing rotor performance. The analyses yielded the following conclusions:

- 1) **Dynamic** blade twist can be utilized to reduce rotor power and improve helicopter performance.
- 2) In hover and low speed forward flight, the rotor power savings by different harmonic twist are substantially small. The effect becomes pronounced in medium to high speed flight.
- 3) Higher harmonic twist usually obtains less power reductions than lower harmonic twist.
- 4) The power reductions by the periodic harmonic twist are substantially small. The zero harmonic twist gives larger benefits than the periodic harmonic twist.
- 5) The helicopter take-off weight can have pronounced influence on the power reductions achieved by the **dynamic** blade twist.

Finally, it is noted that the precise numbers given above are specific to the blade utilized in this work. For a rotor with different planform, airfoils, diameter, etc., the optimum deployment and performance improvement levels may vary.

#### Acknowledgements

This work is supported from the National Natural Science Foundation of China (11472129).

## References

- [1] Gessow, A., "Effects of Rotor-Blade Twist and Plan-Form Taper on Helicopter Hovering Performance," Technical Report NACA 1542, 1947.
- [2] Gessow, A., "Flight Investigation of Effects of Rotor-Blade Twist on Helicopter Performance in the High-Speed and Vertical-Autorotative-Descent Conditions," Technical Report NACA 1666, 1948.
- [3] Arcidiacono, P. and Zincone, R., "Titanium UTTAS Main Rotor Blade," Journal of the American Helicopter Society, Vol. 21, No. 2, 1976, pp. 12-19.
- [4] Fradenburgh, E. A., "Aerodynamic Design of the Sikorsky S-76 SPRIT™ Helicopter," Journal of the American Helicopter Society, Vol. 24, No. 3, 1979, pp. 11-19.
- [5] Bagai, A., "Aerodynamic Design of the X2 Technology Demonstrator™ Main Rotor Blade," the 64th Annual Forum of the American Helicopter Society, Montreal, Canada, April 29-May 1, 2008.
- [6] Chen, P. and Chopra I., "Hover Testing of Smart Rotor with Induced-Strain Actuation of Blade Twist," AIAA Journal, Vol. 35, No. 1, 1997, pp. 6-16.
- [7] Chen, P. and Chopra I., "Wind Tunnel Test of a Smart Rotor Model with Individual Blade Twist Control," Journal of Intelligent Material Systems and Structures, Vol. 8, No. 5, 1997, pp. 414-425.
- [8] Wilbur, M.L., Yeager, P.H. and Langston, C.W., "Vibratory Loads Reduction Testing of the NASA/Army/MIT Active Twist Rotor," Journal of the American Helicopter Society, Vol. 47, No. 2, 2002, pp. 123-133.
- [9] Shin, S., Cesnik, C.E.S. and Hall, S.R., "Closed-Loop Test of the NASA/Army/MIT Active Twist Rotor for Vibration Reduction," Journal of the American Helicopter Society, Vol. 50, No. 2, 2005, pp. 178-194.
- [10] Bernhard, A.P.F. and Wong, J., "Wind-Tunnel Evaluation of a Sikorsky Active Rotor Controller Implemented on the NASA/ARMY/MIT Active Twist Rotor," Journal of the American Helicopter Society, Vol. 50, No. 1, 2005, pp. 65-81.
- [11] Monner, H.P., Opitz, S., Riemenschneider, J. and Weirach, P., "Evolution of Active Twist Rotor Design at DLR," In 49th AIAA/ASME/ASCE/AHS/ASC Structures, Structural Dynamics, and Materials Conference, Schaumburg, IL, 7-10 April 2008.
- [12] Monner, H.P., Riemenschneider, J., Opitz, S. and Schulz, M., "Development of Active Twist Rotors at the German Aerospace Center (DLR)," In 52th AIAA/ASME/ASCE/AHS/ASC Structures, Structural Dynamics, and Materials Conference, Denver, Colorado, 4-7 April 2011.
- [13] Riemenschneider, J. and Opitz, S., "Measurement of Twist Deflection in Active Twist Rotor," Aerospace Science and Technology, Vol. 15, No. 3, 2011, pp. 216-223.
- [14] Yeo, H., "Assessment of Active Control for Rotor Performance Enhancement," Journal of the American Helicopter Society, Vol. 53, No. 2, 2008, pp. 152-163.
- [15] Zhang, Q., Hoffmann, F., and Van Der Wall, B.G., "Benefit Studies for Rotor with Active Twist Control using Weak Fluid-Structure Coupling," In 35th European Rotorcraft Forum, Hamburg, Germany, September 22-25 2009.
- [16] Boyd Jr., D. D., "Initial Aerodynamic and Acoustic Study of an Active Twist Rotor using a Loosely Coupled CFD/CSD Method," In 35th European Rotorcraft Forum, Hamburg, Germany, September 22-25 2009.
- [17] Kang, H., Saberi, H. and Gandhi, F., "Dynamic Blade Shape for Improved Helicopter Rotor Performance," Journal of the American Helicopter Society, Vol. 55, No. 4, 2010, pp. 0320081 - 03200811.
- [18] Jain, R., Yeo, H. and Chipra, I., "Computational Fluid Dynamics-Computational Structural Dynamics Analysis of Active Control of Helicopter Rotor for Performance Improvement," Journal of the American Helicopter Society, 55(4):0420041-04200414, 2010.
- [19] Jain, R., Yeo, H. and Chopra, I., "Examination of Rotor Loads due to On-Blade Active Controls for Performance



- Improvement,” *Journal of Aircraft*, Vol. 47, No. 6, 2010, pp. 2049-2066.
- [20] Peters, D.A. and HaQuang N., “Dynamic Inflow for Practical Application,” *Journal of the American Helicopter Society*, Vol. 33, No. 4, 1988, pp. 64-68.
- [21] Leishman, J. G., *Principles of Helicopter Aerodynamics*, 2nd ed., Cambridge University Press, New York, USA, 2006, pp. 202-209.
- [22] Yeo, H., Bousman, W.G. and Johnson, W., “Performance Analysis of a Utility Helicopter with Standard and Advanced Rotors,” *Journal of the American Helicopter Society*, Vol. 49, No. 3, 2004, pp. 250-270.
- [23] Steijl, R., Barakos, G.N. and Badcock, K., “A framework for CFD analysis of helicopter rotors in hover and forward flight,” *International Journal for Numerical Methods in Fluids*, Vol.51, No. 8, 2006, pp. 819-847.
- [24] Steijl, R. and Barakos, G. N., “Sliding Mesh Algorithm for CFD Analysis of Helicopter Rotor-Fuselage Aerodynamics,” *International Journal for Numerical Methods in Fluids*, Vol. 58, No. 5, 2008, pp. 527-549.
- [25] Steijl, R. and Barakos, G. N., “A Computational Study of the Advancing Side Lift Phase Problem,” *Journal of Aircraft*, Vol. 45, No. 1, 2008, pp. 246-257.
- [26] Hilbert, K. B., “A Mathematical Model of the UH-60 Helicopter,” Technical Report NASA-TM-85890, 1984.
- [27] Davis, S. J., “Pedesign Study for a Modern 4-Bladed Rotor for the RSRA,” Technical Report NASA-CR-166155, 1981.